Biomedicine & Pharmacotherapy 193 (2025) 118773

Contents lists available at ScienceDirect

Biomedicine & Pharmacotherapy

journal homepage: www.elsevier.com/locate/biopha

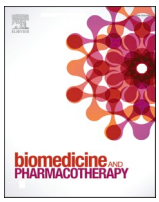

A phenotype-driven data and drug repurposing strategy used to identify potential treatments targeting chondrocyte hypertrophy in osteoarthritis

Judith Veldman [a], Mauricio N. Ferrao Blanco [a,b], Nicole Kops [a], Wendy J.L.M. Koevoet [c], Eric M.J. Bindels [d], Gregory van Beek [d], Remco M. Hoogenboezem [d], Kavitha Sivasubramaniyan [e], Jeroen van Rooij [f], Andrea Lolli [g], Eric Farrell [g], Gerjo J.V.M. van Osch [a,c,h,*]

[a] Department of Orthopaedics and Sports Medicine, Erasmus MC, University Medical Center, Rotterdam, the Netherlands
[b] Princess Máxima Center for Pediatric Oncology, Utrecht, the Netherlands
[c] Department of Otorhinolaryngology, Erasmus MC Cancer Institute, University Medical Center, Rotterdam, the Netherlands
[d] Department of Haematology, Erasmus MC, University Medical Center, Rotterdam, the Netherlands
[e] Galapagos BV, Oegstgeest, the Netherlands
[f] Department of Internal Medicine, Erasmus MC, University Medical Center, Rotterdam, the Netherlands
[g] Department of Oral and Maxillofacial Surgery, Erasmus MC, University Medical Center, Rotterdam, the Netherlands
[h] Department of Biomechanical Engineering, Delft University of Technology, Delft, the Netherlands

ARTICLE INFO

Keywords:
Drug repositioning
Phenotype-driven drug selection
Chondrocyte hypertrophy
Drug discovery
Single-cell RNA sequencing

ABSTRACT

Osteoarthritis (OA) is a common disabling disease for which no effective pharmacological therapy exists. The progression of osteoarthritis is characterized by the loss of homeostasis in the cartilage. Since in the early stages of the disease, a phenotypic switch is seen in which articular chondrocytes become hypertrophic and promote degradation of the cartilage extracellular matrix, targeting this phenomenon might be the key to developing an effective therapy. To accelerate the identification of potential therapy, drug repurposing strategies are used. In this study we have used a novel approach by combining this with the signature reversing principle on single cell transcriptomics data aimed to reverse the hypertrophic phenotype of chondrocytes in osteoarthritic cartilage of patients. We identified 6 drugs predicted to reverse the hypertrophic phenotype of chondrocytes. Subsequent *in vitro* evaluation in human chondrocytes and cartilage explants demonstrated that Cobimetinib, a MEK1/2 inhibitor, indeed reduced chondrocyte hypertrophy-related and catabolic gene expression, such as *SPP1*, *COL10A1*, *MMP13* and *ADAMTS5*, while promoting collagen type 2 and aggrecan gene expression. Finally, single-cell RNA sequencing performed on osteoarthritic cartilage explants exposed to Cobimetinib *ex vivo* confirmed the anti-hypertrophic effect of the identified drug on hypertrophy-related gene expression and velocity analysis shows that cells are diverting toward a homeostatic cartilage cluster. This study is a proof of concept that open-access single cell omics data together with a drug repurposing strategy can identify drugs that target a specific cellular phenotype in diseases like osteoarthritis and could accelerate the drug discovery process.

1. Introduction

Osteoarthritis (OA) is a painful, degenerative disease, which is characterized by progressive structural changes in the joint consisting of cartilage degeneration, synovitis and osteophyte formation. Clinically, this disease presents with chronic pain and loss of mobility and function of the joint [1]. Given the aging society and increasing life expectancy, the societal and economic burden of OA is expected to substantially increase [2]. As the molecular mechanisms within the pathogenesis of osteoarthritis are still not fully understood, pharmaceutical options remain scarce. To date, pharmaceutical treatments for OA are palliative at best. Thus, the development of treatment that not only alleviates symptoms but more importantly could inhibit or potentially even reverse the progression of the disease, will benefit patients who are suffering from OA.

In healthy cartilage, the articular chondrocyte is responsible for the

* Correspondence to: Molewaterplein 40, Rotterdam 3015GD, the Netherlands.
E-mail address: g.vanosch@erasmusmc.nl (G.J.V.M. van Osch).

https://doi.org/10.1016/j.biopha.2025.118773
Received 8 July 2025; Received in revised form 31 October 2025; Accepted 7 November 2025
Available online 11 November 2025

maintenance of the cartilage tissue, consisting of a highly organized network of collagens and proteoglycans, that covers the ends of the long bones [3]. During OA catabolic processes take over, causing cartilage degeneration and chronic synovial inflammation. Most OA drug discovery studies have focussed on the inflammatory component of the disease. However, it has been hypothesized that hypertrophic differentiation of chondrocytes is one of the main drivers in the progression of the disease [4]. In the early stages of the disease, a phenotypic change is observed as a portion of the articular chondrocytes undergo hypertrophic differentiation, which is characterized by increased expression of *COL10A1*, *MMP13*, alkaline phosphatase (ALP) [4,5]. Unraveling and targeting the signaling pathways governing this phenotypic switch could be a key component in generating or identifying an effective therapy. To study and target this subpopulation of chondrocytes, high-resolution techniques such as single-cell RNA sequencing (scRNAseq) could provide detailed insights into their molecular behavior.

The identification of the transcriptomic fingerprint of these cells provides a basis for the reversal of the phenotype. For several other diseases, such as epilepsy [6], muscle atrophy [7] and dyslipidemia [8], drugs have been identified following the signature reversion principle (SRP). This principle assumes that if a drug can reverse an expression pattern linked to a specific phenotype, it can reverse the phenotype itself. Thus, reversing the transcriptomic fingerprint of the hypertrophic chondrocyte could potentially inhibit hypertrophic differentiation or even reverse it. *In silico* network tools such as Ingenuity Pathway Analysis (IPA) can help to identify pathways and upstream regulators governing this phenotype and could therefore facilitate the identification of drugs targeting this process.

To efficiently identify novel druggable targets, drug repurposing strategies are attractive. In an era of exploding omics data generation, enormous databases have been constructed of drugs and small molecules that could be utilized for a more sustainable approach to drug discovery. This strategy is focused on using existing and approved drugs for new therapeutic uses [9] and has proven to be successful in identifying new treatment options for multiple diseases, such as post-menopausal hot flushes [10], Parkinson's [11], Hutchinson-Gilford progeria syndrome [12], and acute myeloid leukemia [13]. As the toxicity and safety of these drugs are already known, repurposing these can save an appreciable amount of time and money usually spent on clinical trials, as this is where most newly developed drugs become stranded [14].

To accelerate drug development and efficiently work with limited resources, we propose a practical and generalizable pipeline integrating a drug repurposing strategy with computational analysis of open-access single cell transcriptomic data. Unlike previous studies that rely on bulk transcriptomic data or single gene-drug correlation, our pipeline prioritizes compounds identified with an integrative approach of phenotype-specific cellular signatures with causal network analysis, providing a mechanistically informed drug discovery framework. Using the hypertrophic chondrocyte phenotype as test case, drugs capable of reversing this transcriptomic phenotype were identified that might have the potential to be applied as therapy for osteoarthritis. Using an *in vitro* model with hypertrophy-induced patient-derived chondrocytes in 3D alginate beads and an *ex vivo* human osteoarthritic cartilage explant model, the potential of the identified drugs to target chondrocyte hypertrophy was tested. The most promising drug underwent initial follow-up analysis, including assessment of toxicity, dose-response and the timing of application. Finally, single-cell RNA sequencing was used to study the effects of this drug on the phenotype of chondrocytes residing in osteoarthritic cartilage, in particular to validate the effect on the hypertrophic chondrocyte cluster.

2. Materials and methods

2.1. Processing of scRNAseq dataset GSE152805

For the identification of the transcriptomic fingerprint of the hypertrophic chondrocyte, an open-access scRNAseq dataset from the Gene Expression Omnibus (GEO) open-access database (GSE152805) was used [15]. This dataset contains data on OA knee articular cartilage of the medial tibial plateau of three patients, containing 11,579 chondrocytes. For data processing, open-access software R (v4.2.2) was utilized, together with the R packages Seurat, dplyr, patchwork, cowplot, ggplot2 and viridis. Quality control was performed on the data of the individual patients, and only cells expressing more than 200 and fewer than 5000 genes and genes expressed in more than 3 cells were used for further analysis. Furthermore, only cells containing less than 5 % mitochondrial RNA were used in further analysis. The datasets were then normalized using LogNormalization, integrated using canonical correlation analysis (CCA) and scaled using ScaleData. Using the top 2000 variable features, a principal component analysis (PCA) was performed. With a JackStraw procedure, the p-value of the top principal components (PCs) was estimated. The first 20 principal components with a p-value below 0.05 were used for dimensionality reduction: Uniform Manifold Approximation and Projection (UMAP). Clusters were obtained with the function FindClusters with a resolution of 0.5. Differentially expressed genes (DEGs) of the hypertrophic chondrocytes compared to the other clusters were identified using the default settings of FindMarkers where ident.1 was set to the hypertrophic cluster 4 and ident.2 was set to NULL. Graphs were created using the ggplot2 and viridis package. For the analysis of the scRNAseq dataset, we generated ourselves, details are described in paragraph *Single-cell RNA sequencing on OA cartilage explants*.

2.2. Key pathway identification and drug selection

Hypertrophic chondrocyte-associated DEGs with a Bonferroni-adjusted p-value lower than 0.05 and a log2 fold change (Log2FC) higher than 0.25 or lower than −0.25 were uploaded to the Ingenuity Pathway Analysis (IPA) software (QIAGEN; version 73620684). From these DEGs, the Log2 Fold change and Bonferroni adjusted p-value were used to perform Core analysis with default settings. Upstream regulators were considered activated at a z-score higher than 2 and inhibited at a z-score lower than −2, as recommended by software developers.

2.3. Chondrocyte and cartilage explant culture

OA cartilage tissue was obtained, with implicit consent, from the waste material of patients undergoing a total knee replacement surgery (16 females, 4 males, mean age±SD = 70.3 ± 6.3 years), with the approval of the medical ethical committees of Erasmus MC Rotterdam and Elisabeth Tilburg Ziekenhuis, Tilburg, protocol number MEC-2021–0595. Donor characteristics can also be found in Supplementary Table 1. The tissue was immersed in NaCl 0.9 % (Sigma Aldrich St. Louis, MO, USA) and stored overnight at 4°C. Details regarding the number of donors per experiment are indicated in the legend of the figures. For explant culture, full-thickness cartilage explants were harvested using a 3 mm biopsy punch, and for chondrocyte isolation, cartilage chips were harvested with a scalpel. Punches and chips were washed twice with 0.9 % NaCl (Sigma Aldrich St. Louis, MO, USA). For the isolation of the chondrocytes, cartilage chips were treated with 2 mg/ml protease from streptomyces griseus (Sigma Aldrich St. Louis, MO, USA) in 0.9 % NaCl for 1.5 h followed by overnight digestion at 37°C with 1.5 mg/ml collagenase B (Roche Diagnostics, Switzerland) in Dulbecco's Modified Eagle's Medium (DMEM) high glucose supplemented with 10 % fetal bovine serum. To obtain a single-cell suspension, a 70 μm filter was used, after which the cell suspension was spun down for 8 min at 250 xg and resuspended in DMEM-LG supplemented with 1 % insulin-transferrin-selenium (ITS fetal mix, BD Biosciences, San Jose, CA, United States), 50 μg/ml gentamicin, and 1.5 μg/ml Amphotericin B (both Gibco, California, USA). Immediately after isolation, the primary chondrocytes were encapsulated in alginate beads. If necessary, cells from multiple donors were pooled to obtain a sufficient number of cells for the

experiment. The cells were re-suspended in 1.2 % (w/v) medium viscosity alginate (Pronova Biopolymer, Drammen, Norway) in 0.9 % NaCl (Sigma Aldrich, St. Louis, MO, USA) at a concentration of 4×10^6 cells/ml. Beads were formed by dripping the suspension in 100 mM CaCl2 (Sigma Aldrich, St. Louis, MO, USA), using a 23-gauge needle. Beads were washed twice with 0.9 % NaCl and once with DMEM low glucose. Based on visual inspection, beads with an aberrant size or structure were discarded. Explants or alginate beads were cultured in DMEM low glucose supplemented with 1 % ITS (BD Biosciences, San Jose, CA, United States), 80 ng/ml L-proline (Sigma Aldrich, St. Louis, MO, USA), 25 μg/ml l-ascorbic acid 2-phosphate (Sigma Aldrich), 50 μg/ml gentamicin, and 1.5 μg/ml Amphotericin B (both Gibco). Going forward, this medium composition will be referred to as "basic medium".

2.4. Exposure of primary chondrocytes to hypertrophy modulator and selected compounds

Alginate beads with primary chondrocytes were cultured for 24 h in basic medium to equilibrate. After 24 h, alginate beads were exposed to 10 ng/ml TGF-β1 and 100 nM of each of the selected drugs or a DMSO 0.01 % as vehicle control dissolved in the abovementioned culture medium for six days. The most promising compound was selected for further testing at various concentrations and various time periods. Culture duration and concentrations are indicated in the results or graphs.

2.5. Drug cytotoxicity assay

After 7 days of culturing in the presence of Cobimetinib, alginate beads were stained using the LIVE/DEAD ® Viability/Cytotoxicity Kit for mammalian cells (Life Technologies) for 40 min at 37°C as described previously [16]. Staining of live and dead cells was visualized by Zeiss fluorescence microscopy at a 6x magnification. For each sample, 10×30 μm Z-stacks were generated. In ImageJ, Z-stacks were merged using maximum intensity projection. Manual selection was performed to remove unfocused edges and channels were split into 8-bit images. Quantification of the live and dead cells was performed on separate FITC and dsRED channels with the "Find Maxima" function in the FIJI software.

2.6. GAG assay

Sulfated glycosaminoglycan (GAG) content and secretion of cartilage explants were assessed with a DMB assay. Conditioned medium was harvested on days 3, 6 and 7. Medium was centrifuged for 8 min at 300 xg and the supernatant was collected. Explants were digested overnight at 56°C in 1 mg/mLproteinase K (Sigma Aldrich, #P2308) in Tris/EDTA buffer containing 1 mM iodoacetamide (Sigma Aldrich, #I6125) and 10 μg/ml pepstatin A (Sigma, #P4265) at pH 7.6. After incubation, Proteinase K was inactivated for 10 min at 95°C. 46 μM 1,9-Dimethylmethylene-Blue (Sigma Aldrich, #341088) was added in a ratio of 1:2 (sample:DMB) and the extinction was measured at 590 nm and 530 nm. Chondroitin 6-sulfate from shark cartilage (Sigma Aldrich, #C4348) was used as a reference.

2.7. Gene expression analysis using PCR

For RNA isolation from alginate beads, the encapsulated cells were harvested by dissolving the alginate using a sodium citrate buffer composed of 150 mM NaCl (Sigma Aldrich, St. Louis, MO, USA), 55 mM Na-citrate (Sigma Aldrich, St. Louis, MO, USA) and 20 mM EDTA 2 H_2O (Sigma Aldrich, St. Louis, MO, USA) and centrifugation at 250 xg. The pellet was resuspended in RLT buffer (Qiagen, Hilden, Germany) containing 1 % beta-mercaptoethanol. RNA isolation from explants was performed by snap freezing in liquid nitrogen and pulverization in a Mikro-dismembrator. The pulverized sample was resuspended in RNA STAT-60 (Tel-Test, Friendswood, TX, USA). 20 % chloroform(Sigma Aldrich, St. Louis, MO, USA) was added to the sample and centrifugation at 12.000 xg for 15 min allowed for RNA isolation from the aqueous layer. Further mRNA purification was performed according to the manufacturer's protocol utilizing the RNeasy Column system (Qiagen, Hilden, Germany) and the concentration was determined with a DeNovix DS-11 spectrophotometer (DeNovix Inc, Wilmington, USA). With the use of the RevertAid First Strand cDNA kit (Thermo Fisher Scientific, Waltham, MA, United States) cDNA was synthesized out of 100 ng RNA. Gene expression was assessed by quantitative Polymerase-Chain Reaction (qPCR) using TaqMan Universal Master Mix (Thermo Fisher, Zürich, Switzerland) or SYBR Green Master Mix (Thermo Fisher, Zürich, Switzerland) on a Bio-Rad CFX96 Real-Time PCR Detection System (Bio-Rad). The primers are listed in Supplementary Table 2. Secreted Phosphoprotein 1 (*SPP1*) and Receptor activator of nuclear factor kappa-B ligand (*RANKL*) primer were purchased as assays-on-demand from BioRad. Data were analyzed by the ΔCt method. Gene expression of primary chondrocytes cultured in alginate beads was normalized to a best keeper index (BKI) consisting of Beta-2-Microglobulin (*B2M*), Glyceraldehyde 3-phosphate dehydrogenase (*GAPDH*), and Ubiquitin C (*UBC*) expression. The fold change was obtained by normalizing the gene expression of each sample to the corresponding average of the samples in the control groups.

2.8. Single-cell RNA sequencing on OA cartilage explants

Cartilage explants were digested by incubation in protease at a concentration of 10 mg/ml for 45 min and subsequently incubated in collagenase B at 4 mg/ml until the explants were completely digested, which was after approximately 4.5 h. Cell pellets were washed with PBS/0.04 % UltraPure BSA. Three donors were pooled per experimental condition. Samples were prepared using 10x genomics chemistry version 3′ v3 and the resulting libraries were sequenced on a Novaseq6000 platform (Illumina, San Diego, CA, USA). Subsequently, FASTQ files were constructed using cellranger mkfastq (version 7.1.0) in combination with blc2fastq (version 2.20.0.422). The resulting FASTQ files were processed using cellranger count (version 7.1.0). The genome version used in processing was GRCh38. Cells were assigned to the correct sample present in the multiplexed pools using vireo (version 0.2.3) in combination with cellsnp-lite (version 1.2.3). Gene expression analysis was performed using R (version 4.3.1). Quality control was performed on the individual patients, by filtering based on thresholds for RNA features (750–6000), RNA counts, and mitochondrial RNA percentage, with additional markers (CD163, CD84, HLA-DRA) used to exclude specific cell types (Supplementary Table 3). Data was normalized using logNormalize and scaled using ScaleData. PCA was performed using the top 20 principal components and subsequent clustering with a resolution of 0.5. The Cobimetinib-treated cells were mapped onto the clustering of the control DMSO-treated cells using FindTransferAnchors and MapQuery. Pseudobulk analysis was performed using an in-house build software pseude [https://github.com/weversMJW/pseude]. Velocity analysis using the dynamical model was performed in python. In order to include splicing information from the counts matrices obtained from cellranger, the `velocyto run10x` pipeline (v0.17.17) is used in python (v3.7.16) together with samtools (v1.9). Velocyto.loom files were processed with scVelo (v0.3.3) and Scanpy (v1.10.3), merged and harmonized to the Seurat-derived cell and UMAP annotations. Genes with fewer than 50 counts were filtered out and 3000 highly variable genes were retained. Log-normalization, PCA analysis (30 pcs) and kNN classification (30 neighbors) was performed. RNA velocity, pseudotime and latent time were first computed on the merged dataset. To account for potential differences in splicing kinetics, the velocity dynamics were recomputed separately for Control and Cobimetinib-treated cells to obtain group-specific pseudotime and latent time.

2.9. Statistical analyses

Biological and technical replicates used in each experiment is stated in the caption of each figure. Statistical evaluation was performed using R software (version 4.2.1). Linear mixed-effects modeling was performed using 'lm()' from the 'stats' package for single donor comparisons and the 'lmer()' function from the 'lmerTest' package for multiple donor comparisons. After fitting the model, two group comparisons were subjected to a *t*-test using the 'lmerTest' package. For multiple comparisons, ANOVA and post hoc Dunnett's test were performed using the 'emmeans()' function from the 'emmeans' package. P-values< 0.05 were considered statistically significant. The drug screening assay and the comparative experiment between Trametinib and Cobimetinib were designed as exploratory assessments and since they did not include multiple independent replicates from different donors, no statistical analysis is shown.

3. Results

3.1. scRNAseq data analyses and drug repurposing strategy based on molecular signature reversing principle identified six potential chondrocyte hypertrophy inhibitors

First, we determined the molecular signature of hypertrophic

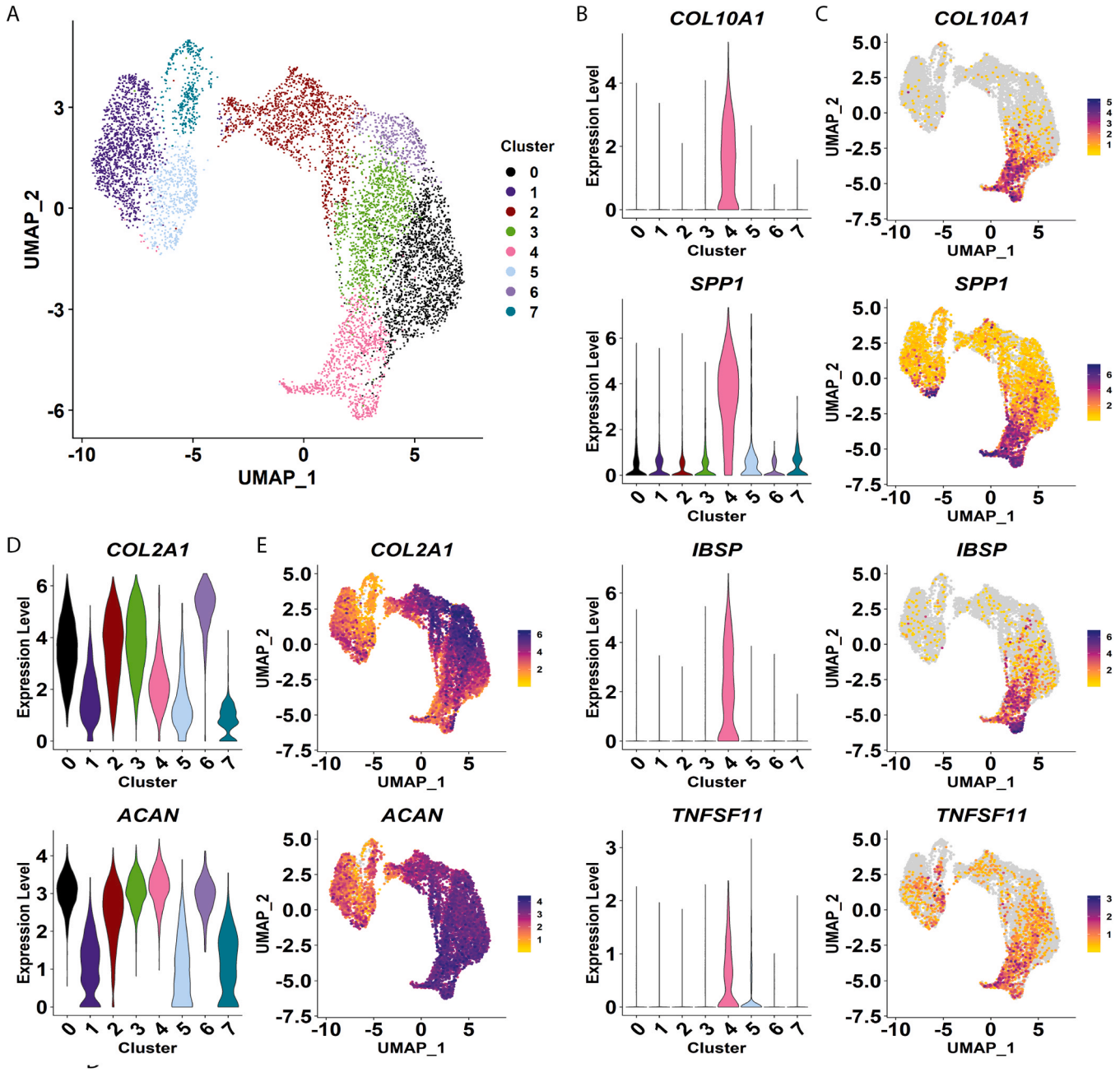

Fig. 1. Analysis of GSE152805, an open-access scRNAseq dataset of chondrocytes from OA cartilage derived from the medial tibia plateau of 3 patients (A) UMAP plot visualizing 8 clusters identified by unsupervised clustering of 7421 chondrocytes. (B) Violin plots showing the expression of hypertrophy-related genes *COL10A1*, *SPP1*, *IBSP* and *TNFSF11* in the separate 8 clusters. (C) UMAP colored by relative gene expression of hypertrophy-related genes *COL10A1*, *SPP1*, *IBSP* and *TNFSF11*. Yellow indicates low expression, whereas purple indicates high expression. (D-E) Violinplots and Featureplots, respectively, of chondrogenic markers *COL2A1* and *ACAN*.

chondrocytes in human osteoarthritic cartilage using publicly available scRNA-seq data [15]. Following quality control and the exclusion of irrelevant cell types, namely VSMCs, ECs, and macrophages (Supplementary Figure 1), 7421 chondrogenic cells were reanalyzed using PCA, clustering, and differential expression analysis. With this analysis, 8 distinct clusters could be identified, each characterized by their most prominent markers (Fig. 1A & Supplementary Table 4). Cluster 4, comprising 12 % of the subset of chondrocytes, was identified as hypertrophic chondrocytes, based on the increased expression of markers related to chondrocyte hypertrophy, such as *COL10A1*, osteopontin (*SPP1*), Integrin Binding Sialoprotein (*IBSP*), Tumor Necrosis Factor Ligand Superfamily Member 11 (*TNFSF11*, also known as Receptor Activator Of Nuclear Factor Kappa B Ligand (*RANKL*)) (Fig. 1B-C and Supplementary Table 4) [17–20]. Furthermore, the hypertrophic chondrocyte cluster was one of the clusters with a relatively low expression of *COL2A1*, although still retaining a high expression of *ACAN* (Fig. 1D-E and Supplementary Table 4), both markers of healthy extracellular matrix (ECM). The complete list of differentially expressed genes (DEGs) (n = 337) of the hypertrophic chondrocytes compared to the other chondrocytes in the dataset was obtained using FindMarkers and used for further analysis (Supplementary Table 5).

According to the signature reversing principle, a drug that would reverse this hypertrophic fingerprint would also reverse the phenotype itself. Therefore, the full transcriptomic signature, in the form of DEGs, of the hypertrophic chondrocyte was used in the Upstream Regulator Analysis of the IPA software. By focussing on upstream regulators, rather than direct gene-drug correlation, drug were selected on their mechanistic plausibility to reverse the disease-relevant phenotype. This resulted in 21 chemicals and drugs that are predicted to be candidate drugs as their z-score is below −2 and are therefore considered significantly 'inhibited' upstream regulators of the hypertrophic chondrocyte-associated DEGs (Fig. 2A and Supplementary Table 6). Combined with a drug repurposing strategy, from this list six compounds were selected for further analysis. Compounds or analogs were excluded if they were either not approved by the FDA/EMA, were not naturally occurring agents, or had been previously studied in the context of OA (Fig. 2A and Supplementary Table 6).

3.2. *In vitro compound screening uncovers a promising compound in targeting hypertrophy-related gene expression*

The six selected compounds were screened in a 3D culture model for human OA chondrocyte hypertrophy. To increase the window to modulate chondrocyte hypertrophy, TGF-β1 was used to stimulate hypertrophy [21], which was confirmed with the increase of several hypertrophic markers, such as *COL10A1* and *RANKL*, upon TGF-β1 treatment (data not shown). Cobimetinib (COB) and Losmapimod (LOS) decreased the expression of *COL10A1* (Log2FC±SD: −0.474 ± 0.129 and −0.744 ± 0.208 respectively) and *SPP1* (Log2FC±SD:-2.361 ± 0.181 and −0.936 ± 0.255 respectively)(Fig. 2B). Furthermore, Cobimetinib decreased multiple other catabolic or hypertrophy-related genes significantly, such as *IBSP* (Log2FC±SD:-1.623 ± 0.482), *RANKL* (Log2FC±SD:-2.077 ± 0.335), *MMP13* (Log2FC±SD:-4.045 ± 0.155), and *ADAMTS5* (Log2FC±SD:-4.111 ± 0.789). In contrast, it increased the expression of anabolic ECM components *COL2A1* and *ACAN* (Log2FC±SD: 4.593 ± 0.338 and 1.930 ± 0.187 respectively). Losmapimod only showed an additional minimal decrease of *MMP13* (Log2FC ±SD:-0.667 ± 0.254), similar to Actinonin (Log2FC±SD:-0.508 ± 0.102). Amantadine, Carbidopa and Regadenoson did not demonstrate any reductive effect on hypertrophy-related gene expression.

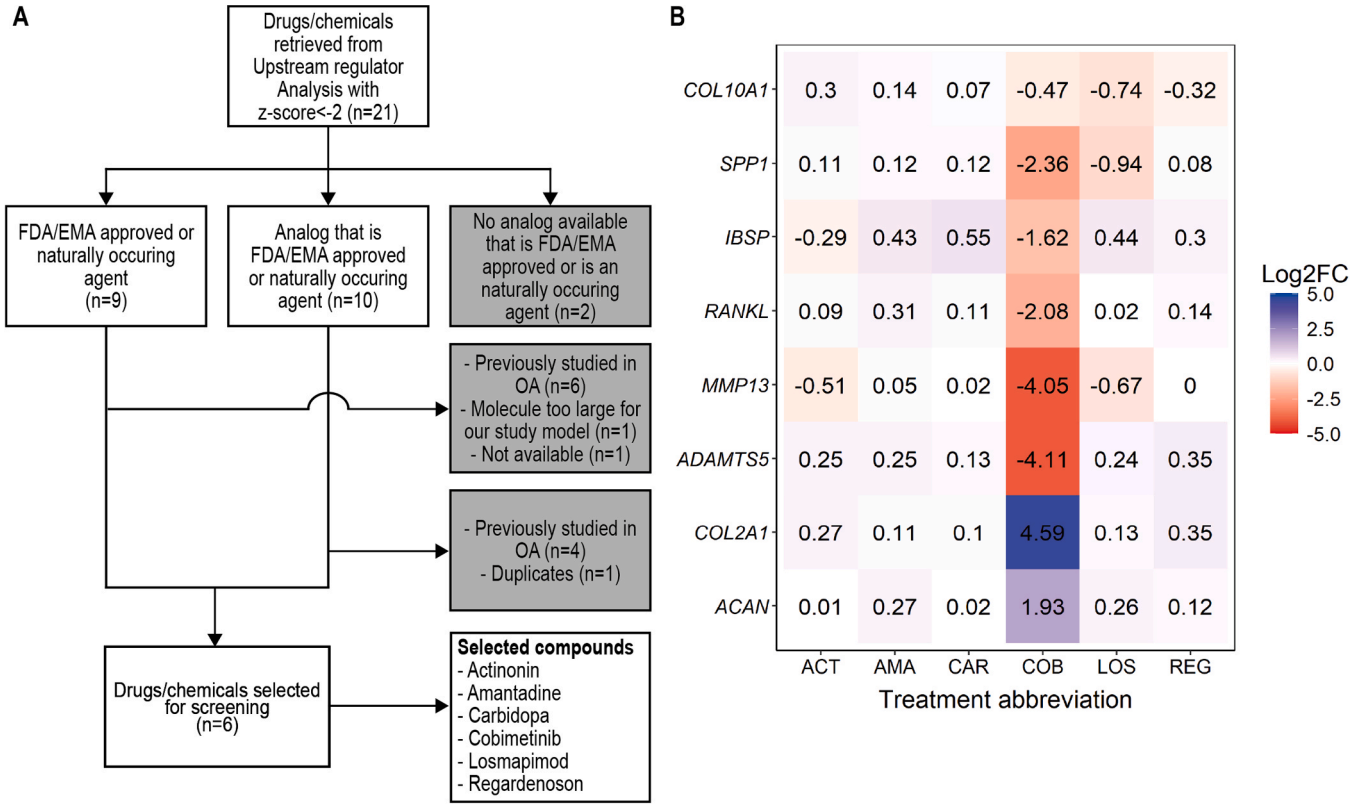

Fig. 2. Combination of pathway analysis and a drug repurposing strategy leads to potential hypertrophy inhibitors. (A) Flow diagram of compound selection retrieved from the Upstream regulators analysis on hypertrophic chondrocyte-associated DEGs in the Ingenuity Pathway Analysis software. (B) mRNA expression determined by qPCR of primary chondrocytes cultured in alginate beads stimulated with 10 ng/ml TGF-β1 and treated with 100 nM of Actinonin (ACT), Amantadine (AMA), Carbidopa (CAR), Cobimetinib (COB), Losmapimod (LOS), Regadenoson (REG) or a vehicle control (DMSO) for 7 days (n = 1, pool of 3 donors). Heatmap displaying Log2 fold change compared to vehicle control. All samples were normalized to best keeper index (BKI) (*GAPDH*, *B2M* and *UBC*) expression.

As Cobimetinib showed the most promising results in this screening, further experiments with Cobimetinib were performed. A dose-response study utilizing Live/Dead staining revealed that Cobimetinib induced toxicity at concentrations of 10 μM or higher (Fig. 3A). In a concentration range from 1 to 1000 nM, treatment with increasing concentrations of Cobimetinib showed an increase in *COL2A1* and *ACAN* expression, while hypertrophy-related genes *RANKL*, *SPP1*, *ADAMTS5* and *MMP13* decreased in a dose-dependent manner (Fig. 3B). Although the highest tested dose of Cobimetinib (1000 nM) slightly increased *COL10A1* expression in one donor, the expression remained relatively stable in the two other donors.

As Cobinmetinib is a MEK inhibitor, we next repeated the study with the drug Trametinib, another MEK inhibitor with distinct pharmacological dynamics [22]. Since Trametinib showed similar results, this suggests the observed effect of Cobimetinib is due to MEK inhibition (Supplementary Figure 2).

3.3. Evaluating sustained effect on chondrocyte phenotype using in vitro chondrocyte culture model

Exploring the potential window of clinical application of Cobimetinib, an experiment was performed investigating different timings of administration in the 3D *in vitro* alginate bead culture model (Fig. 4A and B). Even when Cobimetinib addition was started after 6 days of hypertrophic stimulation with TGF-β1, it showed the ability to decrease the gene expression of *SPP1*, *RANKL*, *MMP13,* and *ADAMTS5* (FC±SD: 0.027 ± 0.009, 0.062 ± 0.085, 0.098 ± 0.077, 0.059 ± 0.031, respectively) alongside the increase of *COL2A1* and *ACAN* (FC±SD: 133.70 ± 48.04, 11.39 ± 1.19, respectively)(Fig. 4A and C). Moreover, upon removing Cobimetinib, the effect of Cobimetinib on the reduction of hypertrophy persisted for at least 7 days even whilst continuously adding TGF-β1 as a hypertrophy stimulus (Fig. 4B and D) (FC±SD: 0.011 ± 0.001 (*SPP1*), 0.080 ± 0.043 (*RANKL*), 0.045 ± 0.015 (*MMP13*), 0.032 ± 0.015 (ADAMTS5), 79.29 ± 34.65 (*COL2A1*), 4.595 ± 1.173 (*ACAN*)).

3.4. Anti-hypertrophic effect confirmed in ex vivo cartilage explant culture model

To study the effects of Cobimetinib in a model where the native extracellular matrix and thus the physiological cellular environmental cues of cartilage are present, an *ex vivo* model was used to expose explants of human osteoarthritic cartilage to Cobimetinib. In this *ex vivo* culture model, Cobimetinib 1000 nM decreased hypertrophy-related genes *COL10A1* (FC±SD: 0.280 ± 0.343), *SPP1* (FC±SD: 0.003 ± 0.002), *RANKL* (FC±SD: 0.014 ± 0.006), *MMP13* (FC±SD: 0.013 ± 0.006) and *ADAMTS5* (FC±SD: 0.021 ± 0.015). Simultaneously, an increase in *COL2A1* (FC±SD: 2.550 ± 1.574) and *ACAN* (FC±SD: 2.260 ± 1.016) was observed. On protein level, no statistical differences were found in the content or release of GAGs, an important ECM component, following treatment with Cobimetinib for 7 days (Fig. 5B and C). Nevertheless, Cobimetinib inhibited NO released into the medium (FC ±SD: 0.708 ± 0.177) (Fig. 5D), which is a contributing factor in cartilage degeneration due to its role in oxidative DNA damage, stimulating MMP production, promoting apoptosis and activating various inflammatory signaling pathways [23]. These findings on both transcriptomic and functional level, indicate that Cobimetinib decreases the catabolic and hypertrophic behavior of the cartilage explants.

3.5. Single-cell RNA sequencing utilized to show changes in phenotypic cellular subsets upon treatment with Cobimetinib

Our data show an anti-hypertrophic and anti-catabolic effect of Cobimetinib in osteoarthritic cartilage at the bulk tissue level. To investigate whether Cobimetinib reduced the number of hypertrophic cells or inhibited the expression of hypertrophy-related genes in general, we conducted single-cell RNA sequencing on cartilage explants treated with or without Cobimetinib. The sequencing yielded 30,742 cells, of which 16,314 remained after quality control and filtering. Eight distinct clusters could be identified (Fig. 6A and Supplementary Table 7), of which cluster 5 was annotated as hypertrophic chondrocytes due to high expression of *COL10A1*, *SPP1* and *IBSP* (Supplementary Figure 3A). Cluster 4 was marked by a high expression of *TMSBX4*, *COL1A1*, *COL1A2* and *COL3A1* (Supplementary Figure 3B) and therefore annotated as fibrotic chondrocytes [15,24]. Although we were able to annotate these two clusters as their markers are consistently reported in the literature, annotation of other chondrocyte populations in scRNAseq data has shown inconsistencies in classification and marker definitions. Therefore, we were unable to assign these clusters to previously described chondrocyte subtypes confidently.

Mapping the Cobimetinib-treated cells onto these clusters revealed significant changes in cell proportions (Fig. 6B). Although the hypertrophic cluster 5 showed a very small increase (Log2FC = 0.513, p = 0.001), clusters 4 and 7 diminished severely (Log2FC = −2.413, p = 0.001 and log2FC=-2.902, p = 0.001). This was also reflected in the pseudobulk analysis, which showed the downregulation of fibrotic markers such as *FN1* (Fig. 6C). Additionally, pseudo-bulk analysis showed *MMP13* and *SPP1* in the top-downregulated markers by Cobimetinib (Fig. 6C), consistent with our bulk PCR data (Fig. 5A). Amongst the most upregulated genes we find *C1QTNF3*, a negative regulator of the NFkB-pathway [25] and *CRYAB*, a promoter of ECM production, while simultaneously inhibiting cartilage degradation [26](Fig. 6C and Supplementary Table 8). Within the hypertrophic cluster the expression of hypertrophic genes *COL10A1*, *SPP1* and *IBSP* decreased and *MMP13,* highly expressed in the fibrotic cluster, was completely abrogated (Fig. 6D). Pro-chondrogenic marker *ACAN* increased across all clusters upon Cobimetinib treatment but remained relatively low in the fibrotic chondrocytes, similar to *COL2A1* expression (Fig. 6D). Although there is no clear decrease in the size of the hypertrophic cluster, processes regarding metal ions, response to oxygen levels and growth regulation are clearly activated in Cobimetinib-treated hypertrophic chondrocytes, while processes regarding cellular movement, differentiation state and TGF-β signaling pathway were clearly downregulated (Supplementary Figure 4A). Furthermore, while the hypertrophic cluster is seemingly one of the terminal differentiation states in the Control dataset, this is less evident in the Cobimetinib treated dataset (Fig. 6E and Supplementary Figure 4B). The velocity pattern in Cobimetinib-treated chondrocytes is deviated from cluster 5 toward cluster 3, which is characterized by high expression of key ECM components such as *COL2A1* and *COL9A1* (Supplementary table 8). Furthermore, pseudotime visualizes the lack of increase in *COL10A1* and *SPP1* expression in when chondrocytes are treated with Cobimetinib, in contrast to *COL2A1* and *ACAN* (Fig. 6E). In conclusion, single-cell RNA sequencing on cartilage explants treated with Cobimetinib demonstrated a reduced expression of hypertrophic marker genes by hypertrophic chondrocytes as well as anti-fibrotic effects due to Cobimetinib treatment.

4. Discussion

This study demonstrates that the use of open-access single cell omics data, pathway analyses and a signature reversing principle combined with a drug repurposing strategy can identify drugs that can target a specific cellular phenotype in osteoarthritis. Six candidate compounds were identified that could potentially target disease-associated chondrocyte hypertrophy. Using an *in vitro* model to screen these six candidates for toxicity and efficacy, we selected Cobimetinib as most promising candidate to target hypertrophy-related phenotype, with a set of hypertrophy-related catabolic markers on PCR. We extended our *in vitro* analyses demonstrating that Cobimetinib not only reduced chondrocyte hypertrophy-related gene expression when administered after hypertrophic stimulation with TGF-β1 but also had a sustained effect after its removal. Additionally, using an *ex vivo* explant culture model,

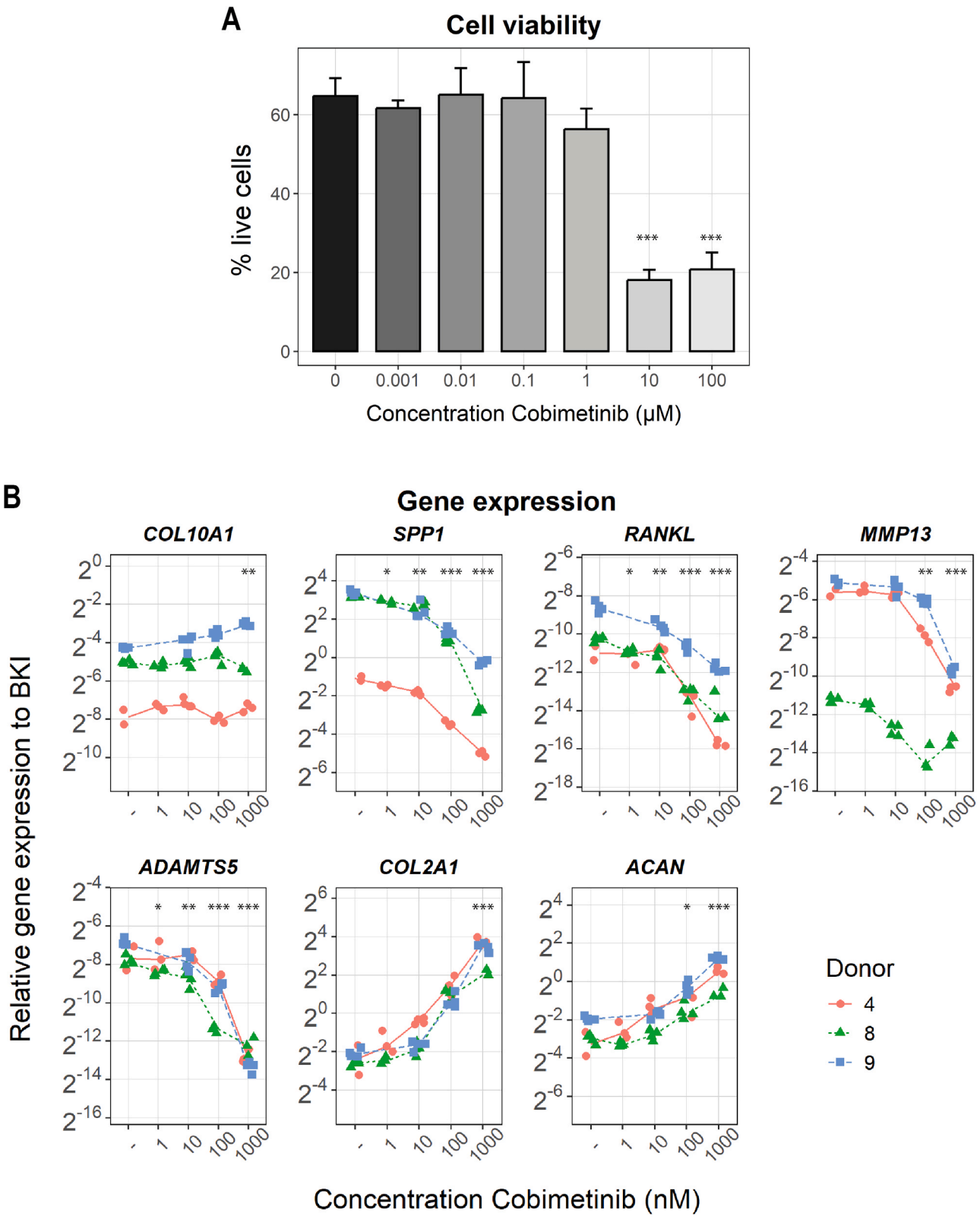

Fig. 3. Cobimetinib has a dose-dependent effect on reducing chondrocyte hypertrophy-related gene expression. (A) Cell viability determined by Live/Dead staining of primary chondrocytes cultured *in vitro* in alginate beads stimulated with 10 ng/ml TGF-β1 and treated with 1nM-100μM Cobimetinib or a vehicle control (0.1 % DMSO) for 7 days (n = 2). Graph shows percentage of live cells. (B) mRNA expression determined by qPCR of primary human chondrocytes cultured in alginate beads stimulated with 10 ng/ml TGF-β1 and treated with 1–1000 nM Cobimetinib or vehicle control (DMSO) for 7 days (n = 3). For donor 3 (blue squares) no data was collected of 1 nM Cobimetinib treatment. Graphs show log2 Fold change of relative gene expression corrected for BKI (*GAPDH*, *B2M*, *UBC*) compared to the vehicle control. Asterisk denotes significant differences compared to control (*: $p < 0.05$, **: $p < 0.001$, ***: $p < 0.0001$).

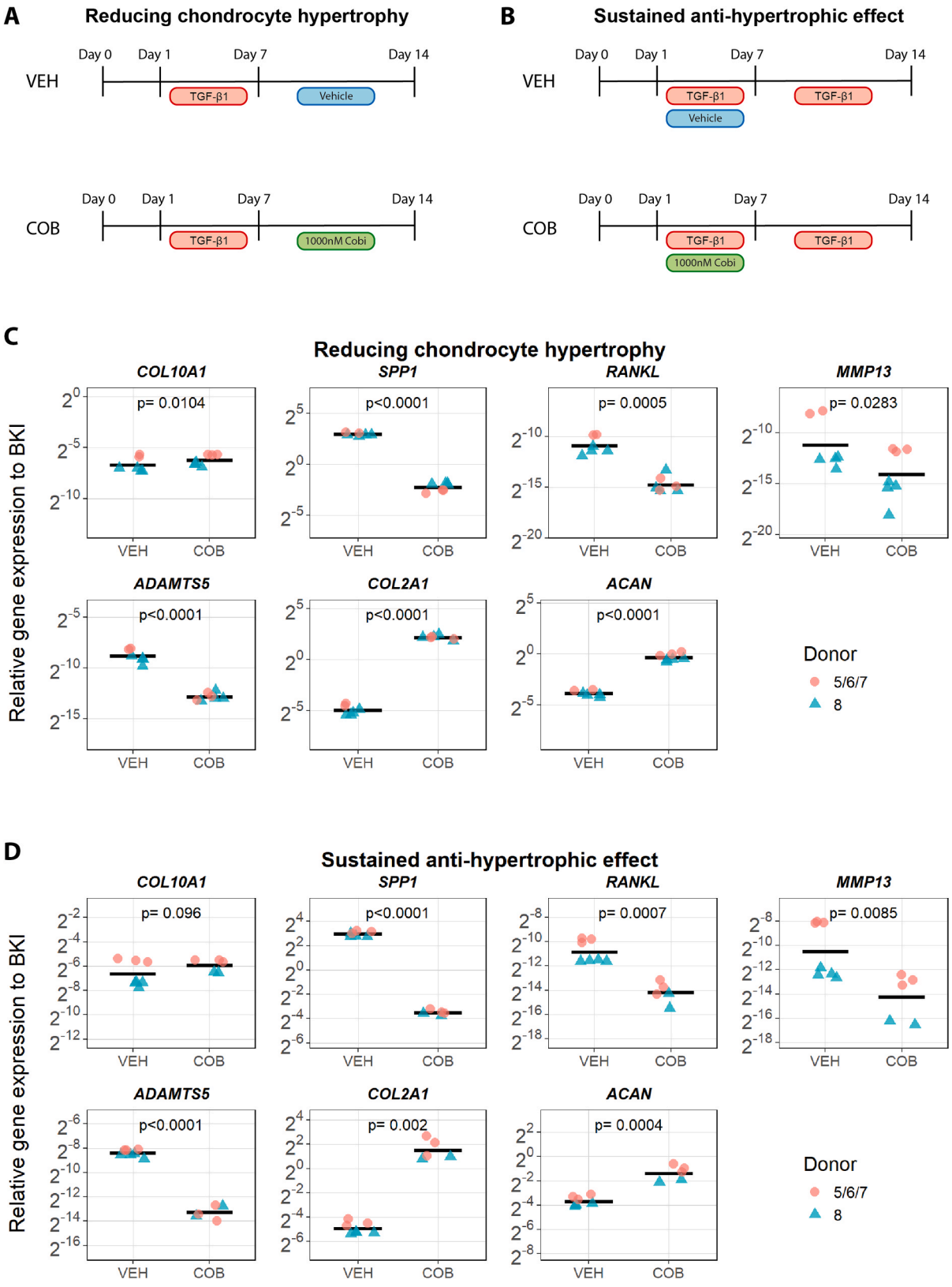

Fig. 4. Cobimetinib shows a reduction of chondrocyte hypertrophy as well as a sustained effect after removal. (A) Experimental set up; primary human OA chondrocytes cultured in an *in vitro* 3D alginate bead culture model for total of 14 days. Chondrocytes were first stimulated to hypertrophy with TGF-β1 for 6 days after which the cells were treated with either 1000 nM Cobimetinib or vehicle control for 7 days (n = 2). Results of this set up are displayed in C. (B) Chondrocytes were simultaneously stimulated towards hypertrophy with TGF-β1 and treated with either 1000 nM Cobimetinib or vehicle control for 6 days, after which stimulation with TGF-β1 was continued for another 7 days. Results of this set up are displayed in D. (C&D) mRNA expression determined by qPCR. Graphs show $2^{-\Delta Ct}$ normalized to the BKI (*GAPDH*, *UBC* and *B2M*). Statistical significance between both conditions is stated within the graph.

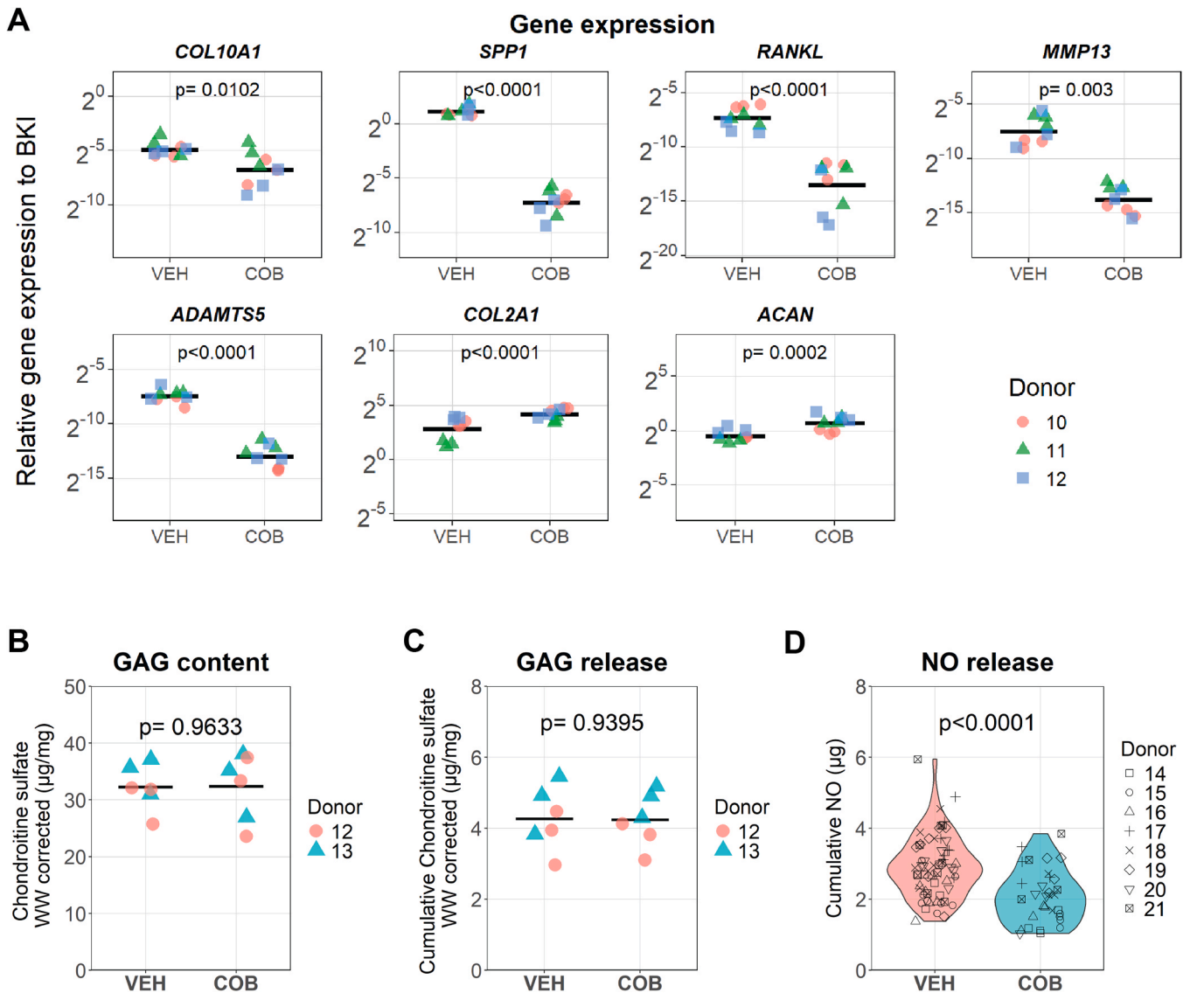

Fig. 5. Cobimetinib has anti-catabolic and pro-anabolic effect in an ex-vivo cartilage model (A) mRNA expression determined by qPCR of *ex vivo* human OA cartilage explant stimulated with 10 ng/ml TGF-β1 and simultaneously treated with 1000 nM Cobimetinib or a vehicle control (DMSO) for 7 days. Results of three donors with 3 technical replicates (circles) containing 4 explants per sample. Graphs show $2^{-\Delta Ct}$ normalized to the BKI (*GAPDH*, *B2M* and *UBC*). (B) GAG content of explants determined by Chondroitin sulfate in explants after 7 days of culture (n = 2). (C) Cumulative GAG release in conditioned medium of above-mentioned explants over 7 days (n = 2). (D) Cumulative NO release in the medium of the abovementioned explants over 7 days. P-values between vehicle control and cobimetinib-treated explants are stated within the graph.

we confirmed the anti-hypertrophic effect of this candidate as well as an inhibition of oxidative stress and inflammation, measured by a decrease in NO release. Finally, single-cell RNA sequencing was used to investigate whether the candidate exerted its effect by reducing the number of hypertrophic cells or by inhibiting the expression levels of hypertrophic-related genes. We demonstrated a reduced expression of hypertrophic marker genes by hypertrophic chondrocytes as well as anti-fibrotic effects due to Cobimetinib treatment. Ultimately, the velocity analysis suggests that Cobimetinib redirects transcriptional dynamics from the hypertrophic state towards a phenotype associated with cartilage homeostasis.

Our approach demonstrates how integrating transcriptomic fingerprints and pathway analyses with a drug repurposing strategy can be used to expedite the process of drug discovery based on targeting a cell phenotype, with chondrocyte hypertrophy as example for OA. Pathway analyses such as IPA are increasingly being used to predict potential targets and this study reaffirms its effectiveness in this regard. Notably, half of the compounds predicted by IPA to function as 'inhibited' upstream regulators, or their analogs, were already associated with OA and several have shown promising effects in reducing OA-related markers and processes [27–30], demonstrating the validity of the approach. Additionally, our initial compound screening revealed promising effects of Losmapimod and, predominantly, Cobimetinib on reducing chondrocyte hypertrophy-related gene expression. Together, these findings provided compelling evidence that this integrative approach is suitable to accelerate drug development for diseases such as OA. Building on existing approaches, this pipeline combines a phenotype-driven and mechanistically-informed route to drug discovery. Specifically identifying FDA and EMA-approved drugs, for further studies exploring the effect on osteoarthritis, could significantly reduce the risk of failure and the cost and time spent on the development of a drug. Importantly, the application of this approach can be extended beyond OA to other diseases that are driven by a distinct cellular phenotype, such as activated pulmonary fibroblasts in pulmonary fibrosis, senescent cells in aging-related disorders or pathogenic microglia in neurodegenerative disorders. Rather than relying on single

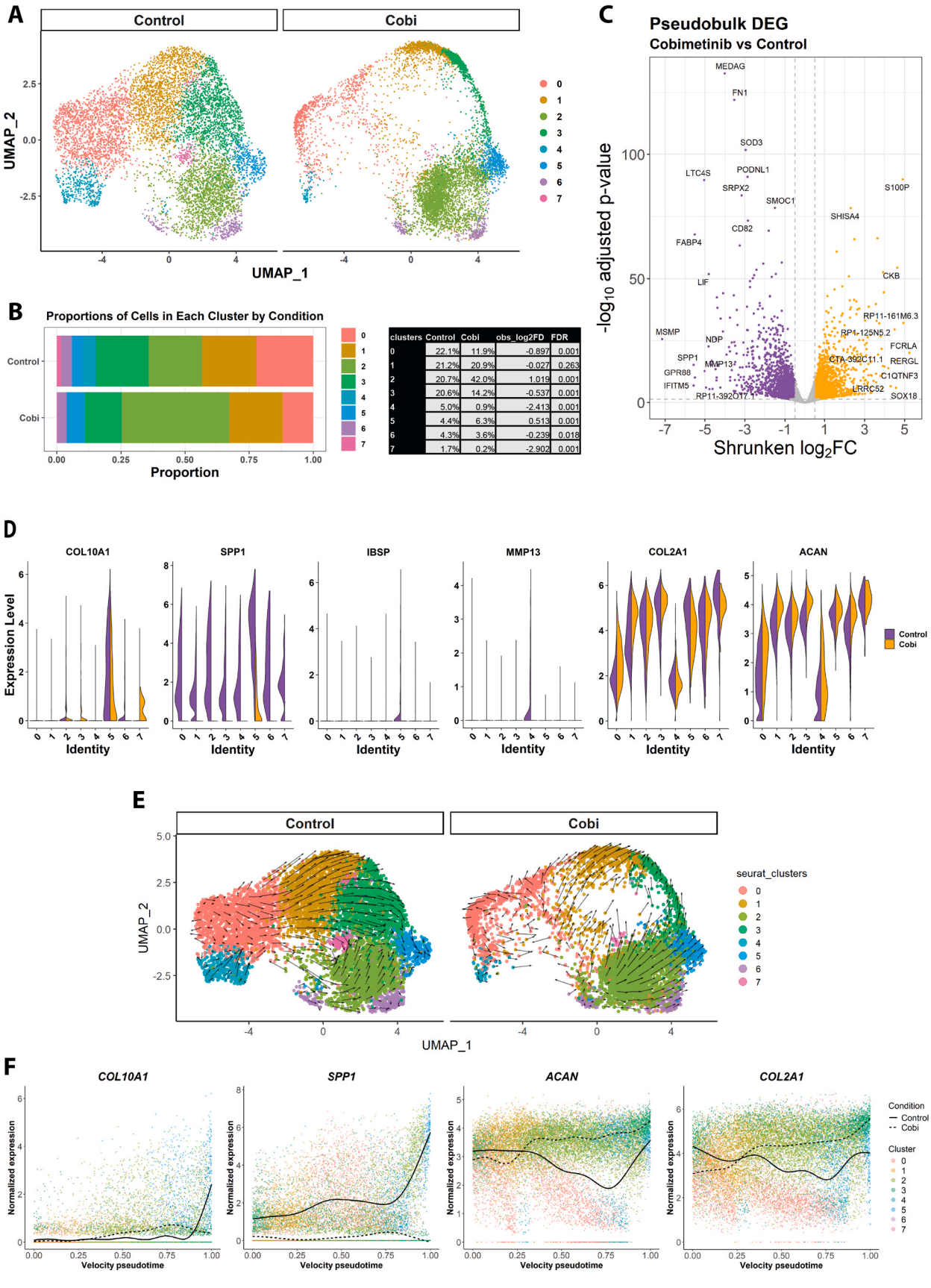

clusters	Control	Cobi	obs_log2FD	FDR
0	22.1%	11.9%	-0.897	0.001
1	21.2%	20.9%	-0.027	0.263
2	20.7%	42.0%	1.019	0.001
3	20.6%	14.2%	-0.537	0.001
4	5.0%	0.9%	-2.413	0.001
5	4.4%	6.3%	0.513	0.001
6	4.3%	3.6%	-0.239	0.018
7	1.7%	0.2%	-2.902	0.001

(caption on next page)

Fig. 6. Cobimetinib shows regulation of fibrotic and hypertrophic chondrocytes on single-cell level. (A) UMAP plot visualizing the clustering of 7827 Control and 8487 Cobimetinib treated chondrocytes. (B) Filled bargraph visualizing the proportions of each cluster in either the Control or Cobimetinib treated samples and table with corresponding proportions and their statistical difference. (C) Volcanoplot of the pseudobulk analysis comparing Cobimetinib vs Control. The names of the top 10 genes with the lowest adjusted p-value and the top 10 highest and lowest shrunken log2FC are displayed in the graph. (D) Split Vlnplots displaying the expression of the hypertrophy markers *COL10A1, SPP1, MMP13, IBSP* and chondrogenic markers *COL2A1* and *ACAN* across the distinct clusters in either the Control chondrocytes or the Cobimetinib-treated chondrocytes. (E) RNA velocity vector field projected on the UMAP embedding of Control or Cobimetinib-treated chondrocytes. Each arrow shows the average velocity direction for cells within a grid bin (30 ×30). Arrow opacity scales with the number of contributing cells and length with the magnitude (speed) of the inferred RNA velocity vector. (F) Expression of hypertrophy markers *COL10A1* and *SPP1*, and chondrogenic markers *COL2A1* and *ACAN* plotted against scaled RNA velocity pseudotime for individual cells. Cells are coloured by Seurat clusters. Smoothed trends are fitted per condition, where the linetype indicates the condition. Pseudotime values were scaled from 0 to 1 separately within each condition, allowing comparison of relative expression dynamics between groups.

gene-drug correlations, this approach identified the full transcriptomic signature of a disease-driving cell population and used prediction models such as IPA to identify drugs that could revert this state, which offers a powerful framework for therapeutic discovery. Moreover, a combination of multiple pathway analysis models could be employed to expand the scope of potential targets and also to improve the accuracy of target selection, making this approach versatile and modifiable to meet the requirements needed across diverse research areas.

The heterogeneity of patient-derived chondrocytes remains a challenge. Increasing evidence on the molecular and clinical level has been found on the existence of multiple OA subtypes [31–33]. While Cobimetinib shows a clear effect in all experiments we performed, we might have diluted relevant effects for other chondrocyte hypertrophy inhibitors on specific OA subtypes as the screening was performed on the pooled cells of three donors. In the pursuit of personalized treatment for OA patients, more knowledge is necessary to diagnose distinct OA endotypes. This would enable the optimization of drug development and clinical studies with drugs that could otherwise potentially fail. Furthermore, the initial screening of six compounds was only performed once and at a concentration of 100 nM. Therefore, these results do not imply that the other compounds are not useful, but the set-up was merely used to select a candidate to enter the *in vitro* experiments. Nevertheless, the possibility remains that different concentrations of the other compounds could still mitigate chondrocyte hypertrophy and to further study these selected compounds, additional experiments could be performed with multiple separate donors and various concentrations.

Cobimetinib, a MEK inhibitor, demonstrated the ability to reverse and prevent TGF-β1-induced chondrocyte hypertrophy. Not only was Cobimetinib able to reverse the hypertrophy-related gene expression, but it also stimulated anabolic chondrogenic markers *COL2A1* and *ACAN*. Multiple studies explored the activation of the MEK/ERK pathway by pro-inflammatory cytokines, oxidative stress or mechanical loading in osteoarthritis causing chondrocyte apoptosis, matrix degeneration or decreased expression of ECM components [34–37]. In this study, we found an anti-hypertrophic effect with Cobimetinib and a similar effect when treated with Trametinib, a MEK inhibitor with distinct pharmacological structure and dynamics compared to Cobimetinib. As an ATP non-competitive kinase inhibitor, Trametinib inhibits both the phosphorylation of MEK and ERK [38], whereas Cobimetinib only inhibits the phosphorylation of ERK [39,40]. Furthermore, Trametinib interacts with the KRS binding surface, while Cobimetinib does not directly interact with this interface, but only binds the allosteric binding pocket [22,41]. This strengthens our claim that the observed effect is due to MEK inhibition, albeit additional molecular targets cannot be completely excluded. While Cobimetinib demonstrated a reduction of most of the tested hypertrophy-related markers, *COL10A1* was occasionally increased in certain donors in the *in vitro* alginate bead model. This effect was not seen when treating *ex vivo* OA cartilage explants or upon treatment with Trametinib or in previous research involving MEK-inhibitor U0126 [42]. This leads us to hypothesize that these findings might be attributed to an off-target effect unique to Cobimetinib in our 3D alginate bead culture model. Future studies should shed light on the dosage, mode, and alternative MEK inhibitors for optimization of the effect. In our efforts to reduce chondrocyte hypertrophy, an unexpected, yet intriguing reduction of fibrotic chondrocytes upon treatment with Cobimetinib was revealed by our scRNAseq dataset. Although not explored further in this study, it is noteworthy given that many efforts in articular cartilage repair strategies ultimately result in the generation of fibrotic cartilage instead of hyaline cartilage [43]. Dedicated future studies should explore this seemingly anti-fibrotic effect of MEK inhibition and investigate the employment of these compounds in cartilage repair attempts.

Previous research has suggested that MEK inhibition could be a promising target in slowing the progression of osteoarthritis, as it not only decreases chondrocyte hypertrophy *in vitro* but also cartilage degeneration, synovial hyperplasia, and inflammation *in vivo* [42,44]. Previous *in vivo* studies on the anti-hypertrophic effect of MEK inhibition only determined the preventative capabilities [42,45,46], without assessing the effect after cartilage degeneration has already occurred. Since the lack of early diagnostic criteria hampers the use of preventative medications in clinical practice, the indications of the potency of Cobimetinib to inhibit hypertrophy are promising. With our models, we demonstrated that, even when Cobimetinib was removed, the effect of decreasing hypertrophy-related gene expression and increasing the expression of healthy ECM components persisted despite continuous hypertrophy stimulation by adding TGF-β1. This is suggestive of sustained phenotypic modulation and could have substantial implications for the clinical implementation of Cobimetinib, as the effect could be maintained while dosing could be intermittent. Future studies exploring epigenetic modifications induced by short-term Cobimetinib treatment could provide deeper insight into the mechanistic basis of this sustained effect. Additionally, Cobimetinib demonstrated its efficacy at a concentration of 100 nM, which is five times lower than the serum concentrations found in patients after treatment with Cobimetinib for BRAFV600-mutated melanoma [47]. With dose optimization, adverse effects seen in the clinical trials for BRAFV600-mutated melanoma could potentially be reduced [48]. To explore the possible applications, follow-up studies in joint-on-a-chip and/or animal models are needed to investigate the optimal dose and mode of treatment with Cobimetinib and its effect on the prevention of progression or the reversal of osteoarthritis, taking into account multiple tissues and processes that are known to be involved in the disease.

Our study focused on developing a generalizable discovery pipeline, leveraging open-access transcriptomic data while nominating approved candidate drugs targeting a specific phenotypic cellular change. This was applied to the hypertrophic chondrocyte during osteoarthritis and resulted in Cobimetinib as a potential therapy. Supplementary to the compounds that were found and evaluated here, the data retrieved from the scRNAseq analysis can indicate many more possible targets for chondrocyte hypertrophy or any other process during OA when using other features of the IPA software or other analytical tools, such as NAViGaTOR or Gene Ontology. This paper emphasizes the proof of concept that computational methods can importantly contribute to the acceleration of drug development when combined with a drug repurposing strategy.

Author contribution

JV designed and performed experiments, analyzed the data and drafted the manuscript. MF, NK and WK assisted in experiments and analyzed data. GB and JR were consulted for the bioinformatics analyses. EB, RH and GB conducted the single-cell RNA sequencing, as well as the data processing and demultiplexing of this dataset. KS and AL helped in discussing the data and experimental setup. MF, EF and GO designed the experimental set-up, discussed the data and revised the manuscript. EF, KS and GO conceived the study. All co-authors have read and approved the manuscript.

CRediT authorship contribution statement

Jeroen van Rooij: Writing – review & editing, Software. **Kavitha Sivasubramaniyan:** Writing – review & editing, Funding acquisition. **Eric Farrell:** Writing – review & editing, Writing – original draft, Validation, Supervision, Resources, Project administration, Methodology, Funding acquisition, Conceptualization. **Andrea Lolli:** Writing – review & editing, Supervision. **Mauricio N. Ferrao Blanco:** Writing – review & editing, Writing – original draft, Supervision, Methodology, Investigation, Conceptualization. **Judith Veldman:** Writing – review & editing, Writing – original draft, Visualization, Validation, Methodology, Investigation, Formal analysis, Data curation, Conceptualization. **Gerjo JVM van Osch:** Writing – review & editing, Writing – original draft, Validation, Supervision, Resources, Project administration, Methodology, Funding acquisition, Conceptualization. **Nicole Kops:** Writing – review & editing, Investigation, Data curation. **Eric MJ Bindels:** Writing – review & editing, Resources, Methodology, Data curation. **Wendy JLM Koevoet:** Writing – review & editing, Investigation, Data curation. **Remco M Hoogenboezem:** Writing – review & editing, Software, Formal analysis, Data curation. **Gregory van Beek:** Writing – review & editing, Software, Formal analysis, Data curation.

Declaration of Generative AI and AI-assisted technologies in the writing process

During the preparation of this work, the authors used BLACKBOX AI in order to optimize and refine script coding in R. After using this tool, the authors reviewed and edited the content as needed and take full responsibility for the content of the published article.

Funding

This work was funded by the Erasmus Medical Center-TKI-LSH (Match) PPP Allowance of Health~Holland (EMCLSH20022). The work is part of the Dutch Arthritis Society Long-term Research Programme INTOarthritis LLP34.

Declaration of Competing Interest

The authors declare the following financial interests/personal relationships which may be considered as potential competing interests: Gerjo J.V.M. van Osch reports financial support was provided by Health Holland. Gerjo J.V.M. van Osch reports financial support was provided by Galapagos NV. Gerjo J.V.M. van Osch reports a relationship with ReumaNederland that includes: funding grants. Gerjo J.V.M. van Osch reports a relationship with Dutch Research Council that includes: funding grants. Gerjo J.V.M. van Osch reports a relationship with TERMIS-EU that includes: board membership. Gerjo J.V.M. van Osch reports a relationship with AO Research Institute Davos that includes: consulting or advisory. Kavitha Sivasubramaniyan was an employee at Galapagos NV during the conduct of this study. Mauricio N Ferrao Blanco reports a relationship with Princess Máxima Center for Pediatric Oncology, Utrecht, the Netherlands that includes: employment. If there are other authors, they declare that they have no known competing financial interests or personal relationships that could have appeared to influence the work reported in this paper.

Acknowledgments

The authors wish to thank the Department of Orthopaedics and Sports Medicine Erasmus MC, University Medical Center and the Department of Orthopaedics of Elisabeth Tilburg Hospital for providing the human samples.

Appendix A. Supporting information

Supplementary data associated with this article can be found in the online version at doi:10.1016/j.biopha.2025.118773.

Data availability

We have shared raw data in the attach file step. ScRNAseq count matrices will be provided through the GEO database.

References

[1] B. Abramoff, F.E. Caldera, Osteoarthritis: pathology, diagnosis, and treatment options, 2020/03/01/, Med. Clin. North Am. 104 (2) (2020) 293–311, https://doi.org/10.1016/j.mcna.2019.10.007.
[2] G.B.D.O. Collaborators, Global, regional, and national burden of osteoarthritis, 1990-2020 and projections to 2050: a systematic analysis for the Global Burden of Disease Study 2021, Lancet Rheuma 5 (9) (Sep 2023) e508–e522.
[3] R. Cancedda, F. Descalzi Cancedda, P. Castagnola, Chondrocyte differentiation, Int Rev. Cytol. 159 (1995) 265–358, https://doi.org/10.1016/s0074-7696(08)62109-9.
[4] P.M. van der Kraan, W.B. van den Berg, Chondrocyte hypertrophy and osteoarthritis: role in initiation and progression of cartilage degeneration? (in eng), Osteoarthr. Cartil. 20 (3) (Mar 2012) 223–232, https://doi.org/10.1016/j.joca.2011.12.003.
[5] T. Saito, et al., Transcriptional regulation of endochondral ossification by HIF-2alpha during skeletal growth and osteoarthritis development, Nat. Med 16 (6) (Jun 2010) 678–686, https://doi.org/10.1038/nm.2146.
[6] N. Mirza, G.J. Sills, M. Pirmohamed, A.G. Marson, Identifying new antiepileptic drugs through genomics-based drug repurposing, Hum. Mol. Genet 26 (3) (Feb 1 2017) 527–537, https://doi.org/10.1093/hmg/ddw410.
[7] S.D. Kunkel, et al., mRNA expression signatures of human skeletal muscle atrophy identify a natural compound that increases muscle mass, Cell Metab. 13 (6) (Jun 8 2011) 627–638, https://doi.org/10.1016/j.cmet.2011.03.020.
[8] A. Wagner, et al., Drugs that reverse disease transcriptomic signatures are more effective in a mouse model of dyslipidemia, Mol. Syst. Biol. 11 (3) (Mar 2015) 791, https://doi.org/10.15252/msb.20145486.
[9] S. Pushpakom, et al., Drug repurposing: progress, challenges and recommendations, Nat. Rev. Drug Discov. 18 (1) (Jan 2019) 41–58, https://doi.org/10.1038/nrd.2018.168.
[10] J.K. Prague, et al., Neurokinin 3 receptor antagonism as a novel treatment for menopausal hot flushes: a phase 2, randomised, double-blind, placebo-controlled trial," (in eng), Lancet 389 (10081) (May 6 2017) 1809–1820, https://doi.org/10.1016/s0140-6736(17)30823-1.
[11] E.J.R. Fletcher, T. Kaminski, G. Williams, S. Duty, Drug repurposing strategies of relevance for Parkinson's disease, Pharm. Res Perspect. 9 (4) (Aug 2021) e00841.
[12] L.B. Gordon, et al., Clinical trial of a farnesyltransferase inhibitor in children with Hutchinson-Gilford progeria syndrome, Proc. Natl. Acad. Sci. USA 109 (41) (Oct 9 2012) 16666–16671.
[13] K. Stegmaier, S.M. Corsello, K.N. Ross, J.S. Wong, D.J. Deangelo, T.R. Golub, Gefitinib induces myeloid differentiation of acute myeloid leukemia, Blood 106 (8) (Oct 15 2005) 2841–2848.
[14] T.T. Ashburn, K.B. Thor, Drug repositioning: identifying and developing new uses for existing drugs," (in eng), Nat. Rev. Drug Discov. 3 (8) (Aug 2004) 673–683, https://doi.org/10.1038/nrd1468.
[15] C.H. Chou, et al., Synovial cell cross-talk with cartilage plays a major role in the pathogenesis of osteoarthritis, Sci. Rep. 10 (1) (Jul 2 2020) 10868, https://doi.org/10.1038/s41598-020-67730-y.
[16] S. Khatab, et al., "MSC encapsulation in alginate microcapsules prolongs survival after intra-articular injection, a longitudinal in vivo cell and bead integrity tracking study," (in eng), Cell Biol. Toxicol. 36 (6) (Dec 2020) 553–570. doi: 10.1007/s10565-020-09532-6[pii]9532 [pii]10.1007/s10565-020-09532-6.
[17] O. Pullig, G. Weseloh, S. Gauer, B. Swoboda, Osteopontin is expressed by adult human osteoarthritic chondrocytes: protein and mRNA analysis of normal and osteoarthritic cartilage, Matrix Biol. 19 (3) (Jul 2000) 245–255.
[18] L. Pesesse, et al., Consequences of chondrocyte hypertrophy on osteoarthritic cartilage: potential effect on angiogenesis, Osteoarthr. Cartil. 21 (12) (Dec 2013) 1913–1923.

[19] E. Tanaka, et al., Vascular endothelial growth factor plays an important autocrine/paracrine role in the progression of osteoarthritis, Histochem Cell Biol. 123 (3) (Mar 2005) 275–281.
[20] W. Hu, Y. Chen, C. Dou, S. Dong, Microenvironment in subchondral bone: predominant regulator for the treatment of osteoarthritis, Ann. Rheum. Dis. 80 (4) (Apr 2021) 413–422.
[21] N.G.M. Thielen, et al., Identification of transcription factors responsible for a transforming growth factor-β-driven hypertrophy-like phenotype in human osteoarthritic chondrocytes, Cells 11 (7) (Apr 5 2022).
[22] Z.M. Khan, et al., Structural basis for the action of the drug trametinib at KSR-bound MEK (in eng), Nature 588 (7838) (Dec 2020) 509–514, https://doi.org/10.1038/s41586-020-2760-4.
[23] H. Jiang, P. Ji, X. Shang, Y. Zhou, Connection between osteoarthritis and nitric oxide: from pathophysiology to therapeutic target, Molecules 28 (4) (2023) 1683. ⟨https://www.mdpi.com/1420-3049/28/4/1683⟩ ([Online]. Available).
[24] Q. Ji, et al., Single-cell RNA-seq analysis reveals the progression of human osteoarthritis, Ann. Rheum. Dis. 78 (1) (Jan 2019) 100–110, https://doi.org/10.1136/annrheumdis-2017-212863.
[25] K. Okada, et al., Hypoxia-inducible factor-1 alpha maintains mouse articular cartilage through suppression of NF-κB signaling," (in eng), Sci. Rep. 10 (1) (Mar 25 2020) 5425, https://doi.org/10.1038/s41598-020-62463-4.
[26] Q. Bao, et al., αB-crystallin (CRYAB) regulates the proliferation, apoptosis, synthesis and degradation of extracellular matrix of chondrocytes in osteoarthritis, 2019/09/15/, Exp. Cell Res. 382 (2) (2019) 111459, https://doi.org/10.1016/j.yexcr.2019.06.004.
[27] L.H. Burton, et al., Systemic administration of a pharmacologic iron chelator reduces cartilage lesion development in the Dunkin-Hartley model of primary osteoarthritis (in eng), Free Radic. Biol. Med 179 (Feb 1 2022) 47–58, https://doi.org/10.1016/j.freeradbiomed.2021.12.257.
[28] W.N. Wan Osman, N.A. Che Ahmad Tantowi, S.F. Lau, S. Mohamed, Epicatechin and scopoletin rich Morinda citrifolia (Noni) leaf extract supplementation, mitigated Osteoarthritis via anti-inflammatory, anti-oxidative, and anti-protease pathways (in eng), J. Food Biochem 43 (3) (Mar 2019) e12755, https://doi.org/10.1111/jfbc.12755.
[29] O. Bruyère, R.D. Altman, J.Y. Reginster, Efficacy and safety of glucosamine sulfate in the management of osteoarthritis: evidence from real-life setting trials and surveys (in eng), Semin Arthritis Rheum. 45 (4) (Feb 2016) S12–S17, https://doi.org/10.1016/j.semarthrit.2015.11.011.
[30] E.H. Mirza, C. Pan-Pan, W.M. Wan Ibrahim, I. Djordjevic, B. Pingguan-Murphy, Chondroprotective effect of zinc oxide nanoparticles in conjunction with hypoxia on bovine cartilage-matrix synthesis (in eng), J. Biomed. Mater. Res A 103 (11) (Nov 2015) 3554–3563, https://doi.org/10.1002/jbm.a.35495.
[31] C. Yuan, et al., Classification of four distinct osteoarthritis subtypes with a knee joint tissue transcriptome atlas, Bone Res. 8 (1) (Nov 12 2020) 38, https://doi.org/10.1038/s41413-020-00109-x.
[32] J.H. Waarsing, S.M. Bierma-Zeinstra, H. Weinans, Distinct subtypes of knee osteoarthritis: data from the osteoarthritis Initiative, Rheumatology 54 (9) (Sep 2015) 1650–1658, https://doi.org/10.1093/rheumatology/kev100.
[33] R. Coutinho de Almeida, et al., Identification and characterization of two consistent osteoarthritis subtypes by transcriptome and clinical data integration, Rheumatol. (Oxf.) 60 (3) (Mar 2 2021) 1166–1175, https://doi.org/10.1093/rheumatology/keaa391.
[34] Q. Chen, X. Kao, Y. Gao, J. Chen, Z. Dong, C. Chen, Increase in NO causes osteoarthritis and chondrocyte apoptosis and chondrocyte ERK plays a protective role in the process, Mol. Biol. Rep. 48 (11) (Nov 2021) 7303–7312, https://doi.org/10.1007/s11033-021-06731-0.
[35] S.Y. Chien, et al., Noggin Inhibits IL-1beta and BMP-2 expression, and attenuates cartilage degeneration and subchondral bone destruction in experimental osteoarthritis, Cells 9 (4) (Apr 10 2020), https://doi.org/10.3390/cells9040927.
[36] N. Hirose, et al., Protective effects of cilengitide on inflammation in chondrocytes under excessive mechanical stress, Cell Biol. Int 44 (4) (Apr 2020) 966–974, https://doi.org/10.1002/cbin.11293.
[37] W. Yin, J.I. Park, R.F. Loeser, Oxidative stress inhibits insulin-like growth factor-I induction of chondrocyte proteoglycan synthesis through differential regulation of phosphatidylinositol 3-Kinase-Akt and MEK-ERK MAPK signaling pathways, J. Biol. Chem. 284 (46) (Nov 13 2009) 31972–31981, https://doi.org/10.1074/jbc.M109.056838.
[38] P. Lito, et al., Disruption of CRAF-mediated MEK activation is required for effective MEK inhibition in KRAS mutant Tumors, 2014/05/12/, Cancer Cell 25 (5) (2014) 697–710, https://doi.org/10.1016/j.ccr.2014.03.011.
[39] A. Singh, Y. Ruan, T. Tippett, A. Narendran, Targeted inhibition of MEK1 by cobimetinib leads to differentiation and apoptosis in neuroblastoma cells, 2015/09/18, J. Exp. Clin. Cancer Res. 34 (1) (2015) 104, https://doi.org/10.1186/s13046-015-0222-x.
[40] G. Hatzivassiliou, et al., Mechanism of MEK inhibition determines efficacy in mutant KRAS- versus BRAF-driven cancers, 2013/09/01, Nature 501 (7466) (2013) 232–236, https://doi.org/10.1038/nature12441.
[41] G.L. Gonzalez-Del Pino, K. Li, E. Park, A.M. Schmoker, B.H. Ha, M.J. Eck, Allosteric MEK inhibitors act on BRAF/MEK complexes to block MEK activation (in eng), Proc. Natl. Acad. Sci. 118 (36) (Sep 7 2021), https://doi.org/10.1073/pnas.2107207118.
[42] I. Prasadam, X. Mao, W. Shi, R. Crawford, Y. Xiao, Combination of MEK-ERK inhibitor and hyaluronic acid has a synergistic effect on anti-hypertrophic and pro-chondrogenic activities in osteoarthritis treatment, J. Mol. Med (Berl.) 91 (3) (Mar 2013) 369–380, https://doi.org/10.1007/s00109-012-0953-5.
[43] A.R. Armiento, M. Alini, M.J. Stoddart, Articular fibrocartilage - why does hyaline cartilage fail to repair? (in eng), Adv. Drug Deliv. Rev. 146 (Jun 2019) 289–305, https://doi.org/10.1016/j.addr.2018.12.015.
[44] J.P. Pelletier, et al., In vivo selective inhibition of mitogen-activated protein kinase kinase 1/2 in rabbit experimental osteoarthritis is associated with a reduction in the development of structural changes, Arthritis Rheum. 48 (6) (Jun 2003) 1582–1593, https://doi.org/10.1002/art.11014.
[45] C.N. Lan, W.J. Cai, J. Shi, Z.J. Yi, MAPK inhibitors protect against early-stage osteoarthritis by activating autophagy, Mol. Med Rep. 24 (6) (Dec 2021).
[46] X. Zheng, et al., Selumetinib - a potential small molecule inhibitor for osteoarthritis treatment, Front Pharm. 13 (2022) 938133.
[47] "Cotellic: EPAR - Product Information," Roche Pharma AG, 003960 - II/0025, 2015. Accessed: 28-07-2022. [Online]. Available: ⟨https://www.ema.europa.eu/en/documents/product-information/cotellic-epar-product-information_en.pdf⟩.
[48] A. Indini, C.A. Tondini, M. Mandala, Cobimetinib in malignant melanoma: how to MEK an impact on long-term survival, Future Oncol. 15 (9) (Mar 2019) 967–977, doi: 10.2217/fon-2018-0659.